PCCP

Cite this: *Phys. Chem. Chem. Phys.*, 2011, **13**, 17729–17736

www.rsc.org/pccp

PAPER

Phosphorescent sensitized fluorescent solid-state near-infrared light-emitting electrochemical cells

Chien-Cheng Ho,[a] Hsiao-Fan Chen,[b] Yu-Che Ho,[a] Chih-Teng Liao,[a] Hai-Ching Su*[a] and Ken-Tsung Wong*[b]

Received 9th June 2011, Accepted 24th August 2011
DOI: 10.1039/c1cp21861a

We report phosphorescent sensitized fluorescent near-infrared (NIR) light-emitting electrochemical cells (LECs) utilizing a phosphorescent cationic transition metal complex $[Ir(ppy)_2(dasb)]^+(PF_6^-)$ (where ppy is 2-phenylpyridine and dasb is 4,5-diaza-9,9′-spirobifluorene) as the host and two fluorescent ionic NIR emitting dyes 3,3′-diethyl-2,2′-oxathiacarbocyanine iodide (DOTCI) and 3,3′-diethylthiatricarbocyanine iodide (DTTCI) as the guests. Photoluminescence measurements show that the host–guest films containing low guest concentrations effectively quench host emission due to efficient host–guest energy transfer. Electroluminescence (EL) measurements reveal that the EL spectra of the NIR LECs doped with DOTCI and DTTCI center at *ca.* 730 and 810 nm, respectively. Moreover, the DOTCI and DTTCI doped NIR LECs achieve peak EQE (power efficiency) up to 0.80% (5.65 mW W^{-1}) and 1.24% (7.84 mW W^{-1}), respectively. The device efficiencies achieved are among the highest reported for NIR LECs and thus confirm that phosphorescent sensitized fluorescence is useful for achieving efficient NIR LECs.

Introduction

Near-infrared (NIR) organic light-emitting devices (OLEDs) could serve as a new class of NIR light sources offering advantages such as light weight, low power consumption, and compatibility with large area and flexible substrates and thus have attracted much attention due to their potential applications in telecommunications, displays and bio-imaging.[1] However, NIR OLEDs[1] typically require sophisticated multi-layer structures and low-work-function cathodes to optimize device efficiencies, influencing their competitiveness with other solid-state NIR emitting technologies. Compared with conventional NIR OLEDs, solid-state NIR light-emitting electrochemical cells (LECs)[2] possess several promising advantages. LECs generally require only a single emissive layer, which can be easily processed from solutions, and can conveniently use air-stable electrodes. The emissive layer of LECs contains mobile ions, which can drift toward electrodes under an applied bias. The spatially separated ions induce doping (oxidation and reduction) of the emissive materials near the electrodes, *i.e.* p-type doping near the anode and n-type doping near the cathode.[3] The doped regions induce ohmic contacts with the electrodes and consequently facilitate the injection of both holes and electrons, which recombine at the junction between p- and n-type regions. As a result, a single-layered LEC device can be operated at very low voltages (close to E_g/e, where E_g is the energy gap of the emissive material and e is elementary charge) with balanced carrier injection, giving high power efficiencies. Furthermore, air-stable metals, *e.g.* Au and Ag, can be used since carrier injection in LECs is relatively insensitive to work functions of electrodes.

Compared with conventional polymer LECs that are usually composed of a neutral emissive conjugated polymer, a salt and an ion-conducting polymer,[2,3] LECs based on cationic transition metal complexes (CTMCs) show several further advantages and have attracted much attention in recent years.[4–28] In such devices, no ion-conducting material is needed since CTMCs are intrinsically ionic. Furthermore, higher electroluminescent (EL) efficiencies are expected due to the phosphorescent nature of CTMCs. A few studies about solid-state NIR LECs (EL peak wavelength longer than 700 nm) based on small-molecule CTMCs[11,13,22,24] and polymers containing pendant CTMC groups[29] have been reported. Nevertheless, compared with visible light-emitting CTMCs, deteriorated photoluminescence quantum yields (PLQYs) of NIR light-emitting CTMCs[11,13,24] are generally obtained due to the energy gap law, which states that the nonradiative decay rates of CTMCs increase as the energy gaps decrease.[12] In addition, self-quenching of chromophores in neat films further limits the device efficiency of NIR LECs based on CTMCs. Thus, neat-film CTMC-based NIR LECs usually exhibited external quantum efficiencies (EQEs)

[a] *Institute of Lighting and Energy Photonics, National Chiao Tung University, Tainan 71150, Taiwan. E-mail: haichingsu@mail.nctu.edu.tw; Fax: +886-6-3032535; Tel: +886-6-3032121-57792*
[b] *Department of Chemistry, National Taiwan University, Taipei 10617, Taiwan. E-mail: kenwong@ntu.edu.tw; Fax: +886-2-33661667; Tel: +886-2-33661665*

lower than 0.1% photon/electron.[11,13,22,24,29] Further improving device efficiencies of NIR LECs would be required for practical applications.

One of the feasible ways to improve device efficiencies of NIR LECs is to employ phosphorescent sensitized fluorescence, which has been proved useful in raising device efficiencies of fluorescent OLEDs to the levels similar to those of phosphorescent OLEDs.[30] In phosphorescent sensitized fluorescence, the heavy-metal center of the phosphorescent host mediates rapid inter-system crossing for efficient intramolecular singlet-to-triplet energy transfer, and thus subsequent effective Förster energy transfer[31] from triplet excitons of the phosphorescent host to singlet excitons of the fluorophore guest, harvesting both singlet and triplet excitons in hosts. Dexter energy transfer[32] from triplet excitons of the phosphorescent host to triplet excitons of the fluorophore guest, which decay nonradiatively, would be insignificant when the guest concentration is low.[30] As a result, device efficiencies of phosphorescent sensitized fluorescent OLEDs could approach those of phosphorescent OLEDs. Since various efficient fluorescent ionic NIR light-emitting laser dyes, which would be compatible with CTMC hosts and thus suitable to serve as guest materials, have been commercially available,[33,34] phosphorescent sensitized fluorescence would be a feasible alternative technique to realize efficient NIR LECs. In this work, we report phosphorescent sensitized fluorescent NIR LECs utilizing a phosphorescent CTMC $[Ir(ppy)_2(dasb)]^+(PF_6^-)$ (where ppy is 2-phenylpyridine and dasb is 4,5-diaza-9,9′-spirobifluorene) as the host and two fluorescent ionic NIR light-emitting dyes 3,3′-diethyl-2,2′-oxathiacarbocyanine iodide (DOTCI) and 3,3′-diethylthiatricarbocyanine iodide (DTTCI) as the guests. Photoluminescence (PL) measurements show that the host–guest films containing low guest concentrations effectively quench host emission due to efficient host–guest energy transfer. EL measurements reveal that the EL spectra of the NIR LECs doped with DOTCI and DTTCI center at *ca.* 730 and 810 nm, respectively. Moreover, the DOTCI and DTTCI doped NIR LECs achieve peak EQE (power efficiency) up to 0.80% (5.65 mW W^{-1}) and 1.24% (7.84 mW W^{-1}), respectively. The device efficiencies achieved are among the highest reported for NIR LECs and thus confirm that phosphorescent sensitized fluorescence is useful for achieving efficient NIR LECs.

Experimental

Materials

Molecular structures of the host and guest materials used in this study are shown in Fig. 1. The host CTMC $[Ir(ppy)_2(dasb)]^+(PF_6^-)$ was synthesized according to the procedures reported in the literature.[15] The fluorescent ionic NIR light-emitting dyes DOTCI and DTTCI (Fig. 1), which have been reported as active materials in efficient NIR dye lasers,[33,34] were used as the guests. DOTCI and DTTCI were purchased from Sigma-Aldrich and were used as received.

Photoluminescent characterization

PL characteristics of DOTCI in ethanol and DTTCI in methanol were recorded at room temperature using 10^{-5} M solutions.

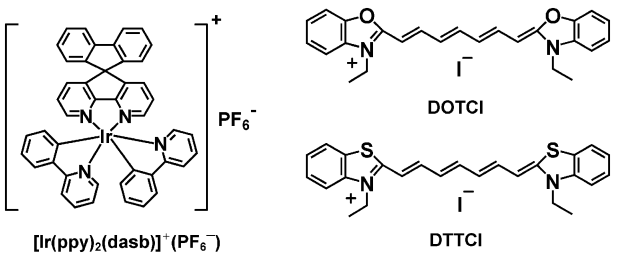

Fig. 1 Molecular structures of $[Ir(ppy)_2(dasb)]^+(PF_6^-)$, DOTCI and DTTCI.

The neat host and host–guest films for PL studies were spin-coated at 3000 rpm onto quartz substrates (1×0.5 cm^2) using mixed solutions (in acetonitrile) of various ratios. Since in LECs, an ionic liquid 1-butyl-3-methylimidazolium hexafluorophosphate $[BMIM^+(PF_6^-)]$ of 20 wt% was added to provide additional mobile ions and to shorten the device response time,[10] PL properties of the $BMIM^+(PF_6^-)$ blended host–guest films were characterized. The mass ratio of solute components of host, guest and $BMIM^+(PF_6^-)$ in acetonitrile solutions for spin coating of the host–guest films containing x wt% guest are $(80 - x)$, x and 20, respectively. The concentrations of all solutions for spin coating are 80 mg mL^{-1}. The thickness of each spin-coated film was *ca.* 200 nm, as measured using profilometry. UV–Vis absorption spectra were recorded using a Hitachi U2800A spectrophotometer. PL spectra were recorded using a Hitachi F9500 fluorescence spectrophotometer. PLQYs for thin-film samples were determined with a calibrated integrating sphere system (HAMAMATSU C9920).

Cyclic voltammetry measurements

Oxidation and reduction potentials of the materials used in this study were determined by cyclic voltammetry (CV, scan rate 100 mV s^{-1}) in acetonitrile solutions (1.0 mM). A glassy carbon electrode and a platinum wire were used as the working electrode and the counter electrode, respectively. All potentials were recorded *versus* the Ag/AgCl (saturated) reference electrode. Oxidation CV was performed using 0.1 M of tetra-*n*-butylammonium hexafluorophosphate ($TBAPF_6$) as the supporting electrolyte. The ferrocenium/ferrocene redox couple in acetonitrile/$TBAPF_6$ showed $E^{0\prime} = +0.47$ V *versus* Ag/AgCl (saturated). For reduction, 0.1 M of tetra-*n*-butylammonium perchlorate (TBAP) in acetonitrile was used as the supporting electrolyte. The ferrocenium/ferrocene redox couple in acetonitrile/TBAP showed $E^{0\prime} = +0.43$ V *versus* Ag/AgCl (saturated). The highest occupied molecular orbital (HOMO) and the lowest unoccupied molecular orbital (LUMO) levels of the materials in solutions were determined according to the equations: $-E_{HOMO} = E_{ox} + 4.8$ eV and $-E_{LUMO} = E_{red} + 4.8$ eV, where E_{ox} and E_{red} are the potentials for the oxidation and reduction processes *vs.* ferrocene.[35]

LEC device fabrication and characterization

Indium tin oxide (ITO)-coated glass substrates (2×2 cm^2) were cleaned and treated with UV/ozone prior to use. A poly(3,4-ethylenedioxythiophene):poly(styrene sulfonate) (PEDOT:PSS) layer was spin-coated at 4000 rpm onto the ITO substrate in air and baked at 150 °C for 30 min. The emissive layer

(~200 nm, as measured by profilometry) was then spin-coated at 3000 rpm from mixed acetonitrile solutions. The mass ratio of solute component and the concentrations of solutions for spin coating of the emissive layers were the same as those used for spin coating of the host–guest films containing $BMIM^+(PF_6^-)$ for PL studies described above. The ionic liquid $[BMIM^+(PF_6)^-]$ was added to enhance the ionic conductivity of thin films and thus to reduce the turn-on time of the LEC device.[10] All solution preparing and spin-coating processes were carried out under ambient conditions. After spin coating, the thin films were then baked at 70 °C for 10 hours in a nitrogen glove box (oxygen and moisture levels below 1 ppm), followed by thermal evaporation of a 100 nm Al top contact in a vacuum chamber ($\sim 10^{-6}$ torr). The electrical and emission characteristics of LEC devices were measured using a source-measurement unit and a Si photodiode calibrated with the Photo Research PR-650 spectroradiometer. All device measurements were performed under a constant bias voltage (2.4 and 2.5 V) in a nitrogen glove box. The EL spectra were taken with a calibrated CCD spectrograph.

Results and discussions

Photoluminescent studies

The previously reported orange-emitting CTMC $[Ir(ppy)_2(dasb)]^+(PF_6^-)$[15,16] was used as the phosphorescent host in this study. As shown in Fig. 2, neat films of the host exhibit orange PL centered at 595 nm. The host shows relatively high PLQYs (~0.32) even in neat films due to superior steric hindrance provided by the bulky diazaspirobifluorene (dasb)-based auxiliary ligand.[15] Furthermore, the peak EQEs (7.1%) of the single-layered host-only devices approximately approach the upper limits that one would expect from the PLQYs of host neat films, when considering an optical out-coupling efficiency of ~20% from a typical layered light-emitting device structure.[15] Since balanced carrier injection could be facilitated by the conductively doped regions near electrodes in LECs, such high EQEs would be attributed to bipolar carrier-transporting characteristics of ppy-based CTMCs,[36] which ensures exciton recombination in the center of the emissive layer and thus prevents exciton quenching in the proximity of electrodes.[37] Hence, phosphorescent $[Ir(ppy)_2(dasb)]^+(PF_6^-)$ is suitable for use as the host material in efficient phosphorescent sensitized NIR LECs. Fluorescent ionic NIR light-emitting dyes DOTCI and DTTCI were used as the guests. As shown in Fig. 2(a) and (b), DOTCI in ethanol solution (10^{-5} M) and DTTCI in methanol solutions (10^{-5} M) exhibit concentrated NIR PL spectra centered at 720 and 780 nm, respectively. Furthermore, DOTCI and DTTCI show intense absorption (molar extinction coefficient $>10^4$ M^{-1} cm^{-1}) at the emission band of the neat host films and consequently host–guest energy transfer would be expected to be feasible (Fig. 2(a) and (b)). Hence, DOTCI and DTTCI are suitable for use as the guest materials in phosphorescent sensitized NIR LECs.

Fig. 3(a) and (b) show the PL spectra of the $[Ir(ppy)_2(dasb)]^+(PF_6^-)$ host films containing 20 wt% $BMIM^+(PF_6^-)$ doped with various guest concentrations of DOTCI and DTTCI, respectively. Since in LECs, an ionic liquid $BMIM^+(PF_6^-)$ of

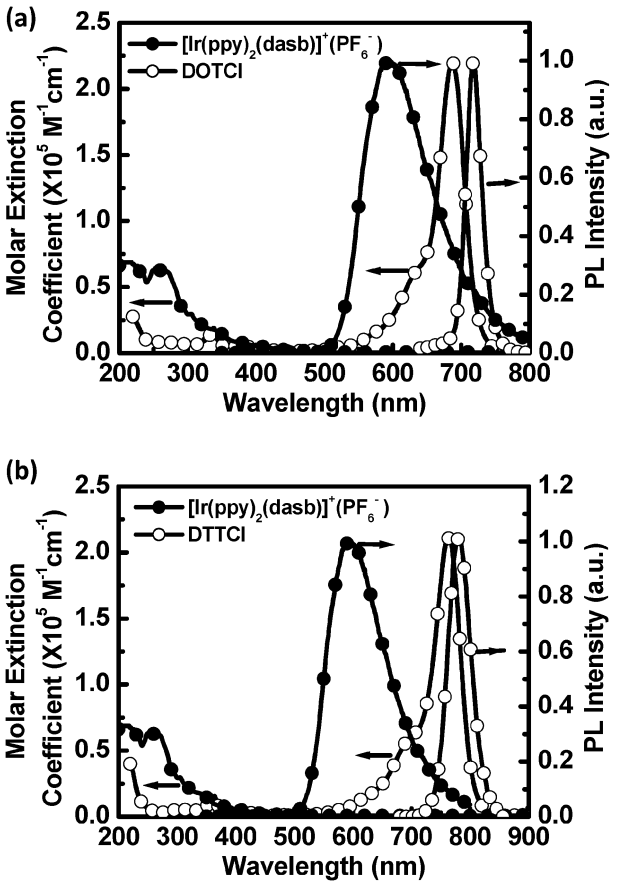

Fig. 2 Absorption spectra of $[Ir(ppy)_2(dasb)]^+(PF_6^-)$ in acetonitrile solution (5×10^{-5} M) along with PL spectra of the $[Ir(ppy)_2(dasb)]^+(PF_6^-)$ neat film and absorption/PL spectra of (a) DOTCI in ethanol solution (10^{-5} M) and (b) DTTCI in methanol solution (10^{-5} M).

20 wt% was added to provide additional mobile ions and to shorten the device response time,[10] PL properties of the $BMIM^+(PF_6^-)$ blended host–guest films were characterized. Calculated Förster radii for the $[Ir(ppy)_2(dasb)]^+(PF_6^-)$/DOTCI and the $[Ir(ppy)_2(dasb)]^+(PF_6^-)$/DTTCI host–guest systems are *ca.* 5.0 and 4.5 nm, respectively. Large Förster radii indicate effective host–guest energy transfer due to high molar extinction coefficients of guests and significant spectral overlap of host emission and guest absorption (Fig. 2(a) and (b)). As shown in Fig. 3(a), guest dominant emission even at low guest concentrations (1.0~1.5 wt%) confirms efficient energy transfer in the $[Ir(ppy)_2(dasb)]^+(PF_6^-)$/DOTCI host–guest system. At similar guest concentrations (1.0–1.2 wt%), the residual host emission in the $[Ir(ppy)_2(dasb)]^+(PF_6^-)$/DTTCI films is more significant (Fig. 3(b)) since the spectral overlap of host emission and guest absorption for the $[Ir(ppy)_2(dasb)]^+(PF_6^-)$/DTTCI host–guest system is smaller than that of the $[Ir(ppy)_2(dasb)]^+(PF_6^-)$/DOTCI host–guest system (Fig. 2(a) and (b)), rendering a relatively lower energy transfer rate. Despite exhibiting residual host emission, comparable host and guest PL emissions at low guest concentrations (*ca.* 1 wt%) still reveal efficient energy transfer in the $[Ir(ppy)_2(dasb)]^+(PF_6^-)$/DTTCI host–guest system (Fig. 3(b)). Compared with both guests in dilute solutions (Fig. 2(a) and (b)), bathochromic shift and broadened full width at half maximum (FWHM) of the PL spectra for both guests in

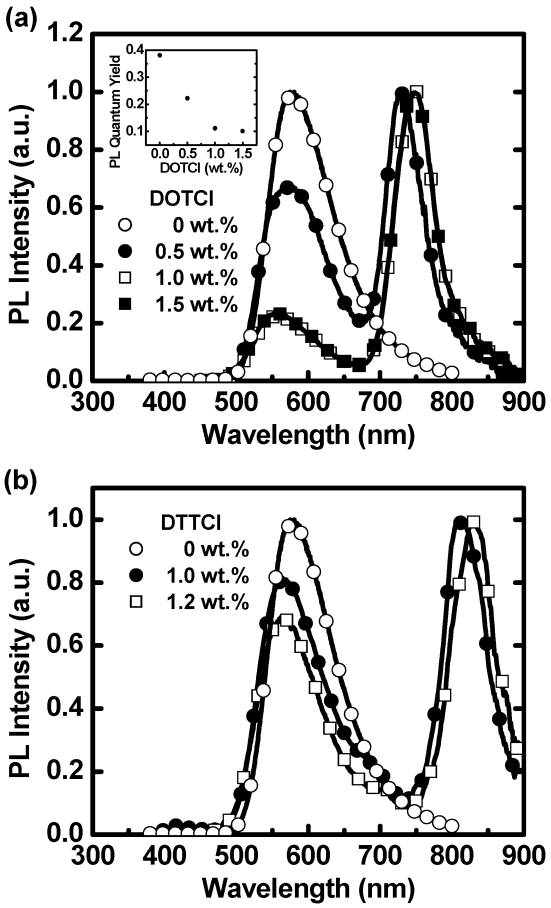

Fig. 3 PL spectra of the $[Ir(ppy)_2(dasb)]^+(PF_6^-)$ host films containing 20 wt% $BMIM^+(PF_6^-)$ doped with various guest concentrations of (a) DOTCI and (b) DTTCI. Inset of Fig. 3(a): photoluminescence quantum yields *vs.* DOTCI concentrations of the $[Ir(ppy)_2(dasb)]^+(PF_6^-)$/DOTCI films.

solid-state host–guest films were observed (Fig. 3(a) and (b)) and would be rationally attributed to enhanced intermolecular interactions of guests in the condensed phase. Increasing guest concentration leads to more pronounced bathochromic shift associated with enhanced solid-state salvation,[38] but the FWHM of the PL spectra remains almost unchanged (Fig. 3(a) and (b)).

Since some residual host emission exists in the PL spectra of the host–guest films (Fig. 3(a) and (b)), it is difficult to determine exact PLQYs of the guests doped in the host films at low concentrations. To eliminate the effect of host emission on estimating the PLQYs of the guests, measuring PLQYs of guest molecules dispersed in an inert host matrix, which is usually non-polar, has commonly been adopted.[15,18,20,25,26] However, ionic dyes have been shown to exhibit significantly different photophysical properties in media with different polarities.[26] Large difference in polarity between the commonly used non-polar inert matrix and a highly polar CTMC host would lead to inaccurate estimation of the PLQYs of the guests. Therefore, to exclude polarity effect, the upper limits of the PLQYs of the guests at low concentrations can still be estimated by measuring the PLQYs of the host–guest films exhibiting relatively insignificant host emission. When the host emission becomes comparable with the guest emission, contribution of PL emission from the host cannot be ignored and thus the estimation of PLQYs of the guests would be inaccurate. Doping-concentration dependent PLQYs of the host–guest films containing DOTCI are depicted in the inset of Fig. 3(a). The overall PLQYs, which contain both host and guest emission, of the host–guest films decrease as the guest concentration increases since the guest emission, which exhibits a lower PLQY than the host emission, gradually dominates PL emission *via* efficient host–guest energy transfer at relatively higher guest concentrations. At guest concentrations >1 wt%, most of the PL emission (*ca.* 80%) of the host–guest films comes from the guest (Fig. 3(a)) and thus the upper limit of PLQY of DOTCI dispersed in the solid-state CTMC host is estimated to be *ca.* 0.10 (the inset of Fig. 3(a)). Compared with the PLQY of DOTCI in dilute solutions (0.28),[33] the lowered PLQY of DOTCI in solid-state films (upper limit is only 0.10) would be ascribed to self-quenching effect and/or difference in environmental polarity.[26] Nevertheless, such solid-state PLQY of the NIR emitting dye is still much higher than those of previously reported NIR emitting CTMCs in dilute solutions.[11,13,24] For the host–guest films doped with DTTCI at *ca.* 1 wt%, the residual host emission (Fig. 3(b)) is comparable with the guest emission and thus would lead to significant overestimation of the upper limit of PLQY of DTTCI dispersed in the solid-state CTMC host. Thus, the method used to estimate the upper limit of PLQY of DOTCI cannot be performed for estimating the upper limit of PLQY of DTTCI. However, similar or even higher solid-state PLQYs of DTTCI as compared to those of DOTCI could be expected due to its higher PLQYs in dilute solutions (0.38).[34] In view of the above results, both $[Ir(ppy)_2(dasb)]^+(PF_6^-)$/DOTCI and $[Ir(ppy)_2(dasb)]^+(PF_6^-)$/DTTCI host–guest systems are capable of offering more efficient NIR PL emission than previously reported CTMCs used in NIR LECs and thus would be beneficial in phosphorescent sensitization for improving device efficiencies of NIR LECs.

EL characteristics of the NIR LECs

To clarify the EL properties of the phosphorescent sensitized system, EL characteristics of the NIR LECs containing various guest concentrations were measured and are summarized in Table 1. The NIR LECs have the structure of ITO/PEDOT:PSS (30 nm)/emissive layer (200 nm)/Al (100 nm), where the emissive layer doped with x wt% guest contains host ($[Ir(ppy)_2(dasb)]^+(PF_6^-)$), guest (DOTCI or DTTCI) and $BMIM^+(PF_6^-)$ in the mass ratio of $(80 - x)$, x and 20, respectively. The ionic liquid $BMIM^+(PF_6^-)$ was added to provide additional mobile ions and to shorten the device response time.[10] The EL spectra of the NIR LECs doped with DOTCI (1.0–1.5 wt%) and DTTCI (1.0–1.2 wt%) under 2.4 V are shown in Fig. 4(a) and (b), respectively. Predominant NIR EL was achieved at low guest concentrations and the EL spectra of the NIR LECs doped with DOTCI and DTTCI center at *ca.* 730 and 810 nm, respectively. Compared with PL (Fig. 3(a) and (b)), the relative intensity of the residual host emission is lower in EL and increases as the bias increases (*e.g.*, EL spectra at 2.5 V shown in Fig. 5(a) and (b)). These results could be understood by energy level alignments of the

Table 1 Summary of the NIR LEC device characteristics

Device guest (concentration)	Bias/V	$\lambda_{max,\ EL}$[a]/nm	t_{max}[b]/min	L_{max}[c]/μW cm^{-2}	$\eta_{ext,\ max}$[d] (%)	$\eta_{p,\ max}$[e]/mW W^{-1}
DOTCI (1.0 wt%)	2.4	730	600	0.58	0.80	5.65
	2.5	729	530	2.42	0.93	6.43
DOTCI (1.5 wt%)	2.4	730	600	0.29	0.50	3.45
	2.5	729	330	2.13	0.66	4.68
DTTCI (1.0 wt%)	2.4	810	580	1.64	1.24	7.84
	2.5	805	430	8.19	1.49	10.16
DTTCI (1.2 wt%)	2.4	810	1430	1.71	1.11	6.79
	2.5	808	880	6.86	1.09	6.91

[a] EL peak wavelength. [b] Time required to reach the maximal light output of devices. [c] Maximal light output achieved at a constant bias voltage. [d] Maximal external quantum efficiency achieved at a constant bias voltage. [e] Maximal power efficiency achieved at a constant bias voltage.

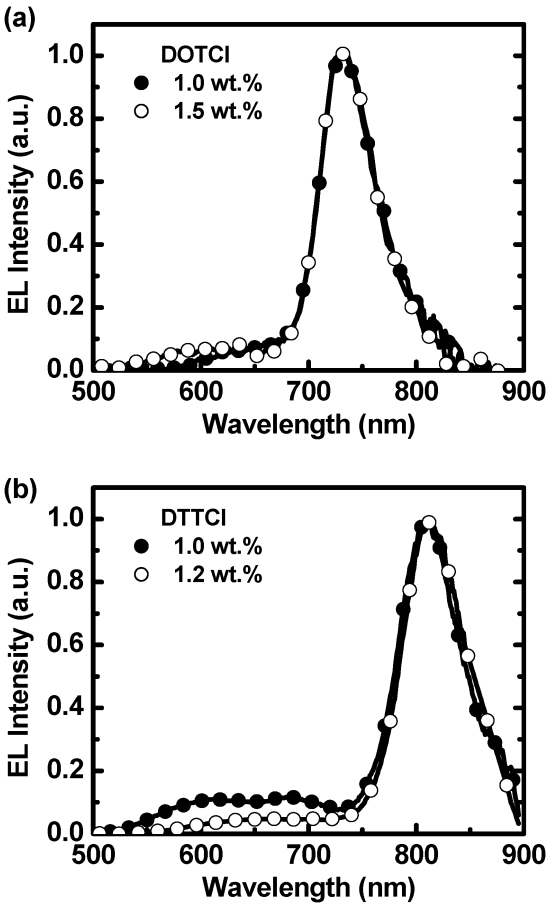

Fig. 4 EL spectra of the NIR LECs doped with (a) DOTCI (1.0–1.5 wt%) and (b) DTTCI (1.0–1.2 wt%) at 2.4 V.

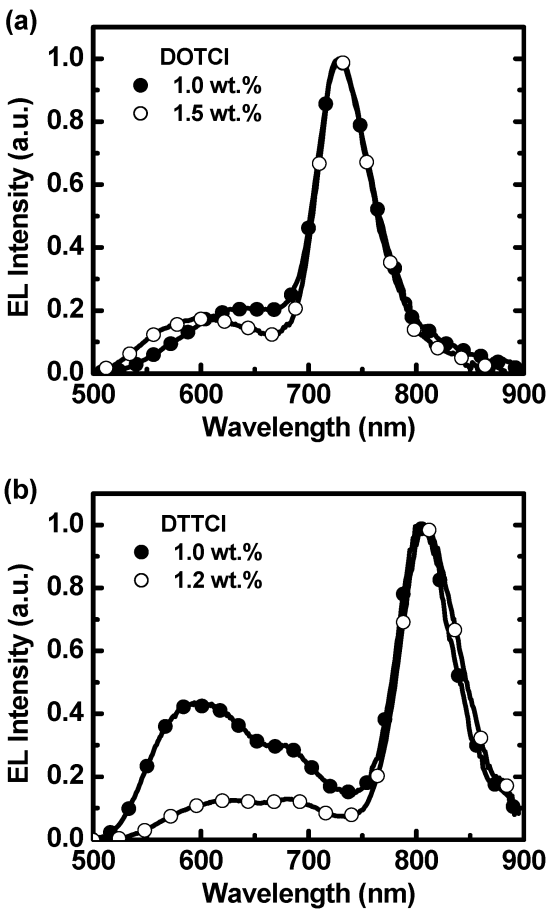

Fig. 5 EL spectra of the NIR LECs doped with (a) DOTCI (1.0–1.5 wt%) and (b) DTTCI (1.0–1.2 wt%) at 2.5 V.

host and guest molecules (estimated by cyclic voltammetry) depicted in Fig. 6. For host–guest LECs, electrochemically doped regions of the emissive layer result in ohmic contact with metal electrodes and consequently facilitate carrier injection onto both the host and the guest. Hence, both exciton formation on the host followed by host–guest energy transfer and direct exciton formation on the guest induced by charge trapping contribute to the guest emission. At lower biases, such energy level alignments (Fig. 6) favor carrier injection and trapping on the smaller-gap guests, resulting in direct carrier recombination/exciton formation on the guest (rather than host–guest energy transfer). Therefore, larger fractions of guest emission are observed at lower biases. As bias increases, carrier injection onto the host and subsequent host–guest energy transfer would be facilitated, resulting in enhanced host emission (Fig. 5(a) and (b)). Although the energy levels of the host and the guest materials in solid-state films cannot be exactly obtained from the estimation of CV measurements in solutions, bias-dependent EL spectra can still be attributed to carrier trapping due to a large offset in energy levels between the host and the guest molecules.

The time-dependent light output and current density under constant biases of 2.4 and 2.5 V for the NIR LECs doped with DOTCI (1.0 wt%) and DTTCI (1.0 wt%) are shown in

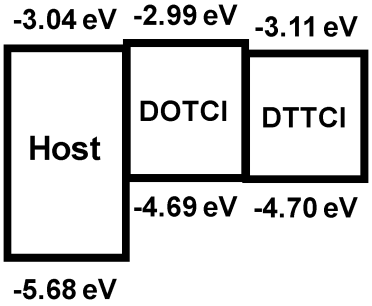

Fig. 6 The energy level diagram of the host ($[Ir(ppy)_2(dasb)]^+(PF_6^-)$) and the guest (DOTCI and DTTCI) molecules.

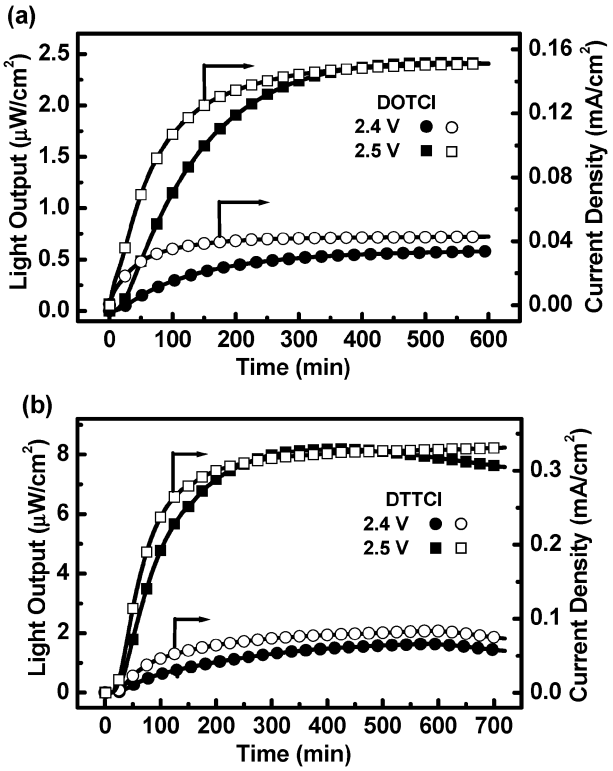

Fig. 7 Light output (solid symbols) and current density (open symbols) as a function of time under a constant bias voltage of 2.4 and 2.5 V for the NIR LECs doped with (a) DOTCI (1.0 wt%) and (b) DTTCI (1.0 wt%).

Fig. 7(a) and (b), respectively. Both devices showed similar trends in time-dependent light output and current density. After the bias was applied, light output and current density first gradually rose and then stayed rather constant. Delayed EL response is associated with the time needed for counterions in the LECs to redistribute under a bias. For the case of the host $[Ir(ppy)_2(dasb)]^+(PF_6^-)$ films, redistribution of the anions (PF_6^-) leads to formation of a region of Ir(IV)/Ir(III) complexes (p-type) near the anode and a region of Ir(III)/Ir(II) complexes (n-type) near the cathode.[8] With the formation of p- and n-regions near the electrodes, carrier injection is enhanced, leading to a gradually increasing device current and light output. A higher bias accelerates accumulation of mobile ions for accomplishing conductive doping and thus shortens the device response time (Table 1).

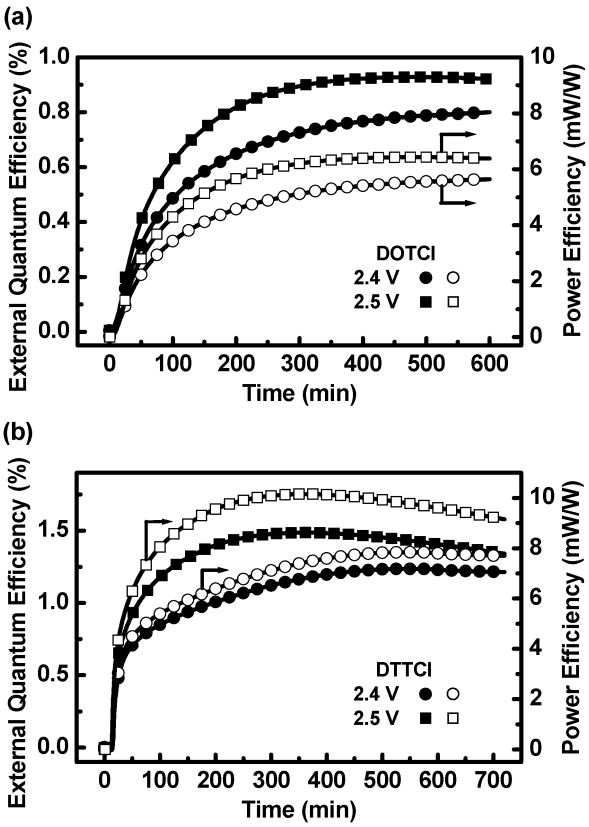

Fig. 8 External quantum efficiency (solid symbols) and power efficiency (open symbols) as a function of time under a constant bias voltage of 2.4 and 2.5 V for the NIR LECs doped with (a) DOTCI (1.0 wt%) and (b) DTTCI (1.0 wt%).

Corresponding time-dependent EQEs and power efficiencies of the NIR LECs doped with DOTCI (1.0 wt%) and DTTCI (1.0 wt%) are shown in Fig. 8(a) and (b), respectively. Both devices exhibited similar time evolution in device efficiencies. When a forward bias was just applied, the EQE was rather low due to unbalanced carrier injection. During the formation of the p- and n-type regions near electrodes, the balance of the carrier injection was improved and the EQE of the device thus increased rapidly. The peak EQE (power efficiency) of the NIR LECs doped with DOTCI (1.0 wt%) and DTTCI (1.0 wt%) at 2.4 V, under which both devices exhibited EL predominantly in the NIR region, are 0.80% (5.65 mW W^{-1}) and 1.24% (7.84 mW W^{-1}), respectively. Higher device efficiencies of LECs doped with DTTCI are consistent with the PLQY of DTTCI in dilute solutions (0.38)[34] is higher than that of DOTCI (0.28).[33] Slight increase in the device efficiency at a higher bias (2.5 V) for both devices (Table 1) results from enhanced residual host emission (Fig. 5), which is more efficient than guest emission. To the best of our knowledge, these device efficiencies are among the highest values reported for the NIR LECs and thus indicate that phosphorescent sensitized fluorescence is useful for achieving efficient NIR LECs. Such high device efficiencies are obtained at bias voltages approaching the electrochemical band gap of the host CTMC (~2.6 V) in solutions (the energy gap in films is usually smaller than that in solutions due to the environmental polarization), at which the LECs show better stability than at higher bias voltages.[15]

Further increase in bias voltages will result in higher brightness and faster response at the expense of LEC device stability, as commonly observed in LECs.[5,9,15,16,19] Thus, we chose bias voltages of 2.4 and 2.5 V, which are lower than those used in reported NIR LECs,[11,13,22,24,29] to demonstrate the advantages of phosphorescent sensitized NIR LECs.

The maximal EQE achieved from the NIR LECs doped with DOTCI is 0.80%. This result is significantly higher than the upper limit by *ca.* 0.50% estimated from a typical layered all-fluorescent device containing an emissive layer with a PLQY comparable with that of DOTCI (0.10) and an optical out-coupling efficiency of ~20%. It confirms efficient phosphorescent sensitized fluorescence in LEC devices, which enables harvesting host triplet excitons *via* Förster energy transfer[31] from triplet excitons on the phosphorescent molecules to singlet excitons on the fluorophores.[30] However, the maximal EQE obtained is still lower than the value (*ca.* 2.0%) one could expect from a typical layered all-phosphorescence device containing an emissive layer with a similar PLQY. Such phenomena suggest two possible exciton loss mechanisms: Dexter energy transfer[32] and/or direct carrier trapping to form triplet excitons on guest molecules. Dexter energy transfer takes place between host triplets and guest triplets when the guest concentration increases, which would degrade the EL efficiency when occurring.[30] Direct carrier trapping results in formation of triplet excitons on guest molecules directly and would degrade device efficiency as well. Carrier trapping impedes carrier transport and thus lowers the device current of the host–guest LECs under the same bias voltage. This phenomenon would be significant when a large difference in energy gaps between the host and the guest molecules exists. Although the energy levels of the host and the guest materials estimated from CV data in solutions (Fig. 6) may not exactly reflect those in solid-sate films due to polarization effect, a large difference in energy gaps between the host and the guest molecules would still be capable of inducing either hole or electron trapping in the host–guest films. As shown in Fig. 9, the device current densities of the host–guest LECs are indeed lower than those of the host-only devices under the same bias voltages, manifesting carrier trapping in the host–guest devices.

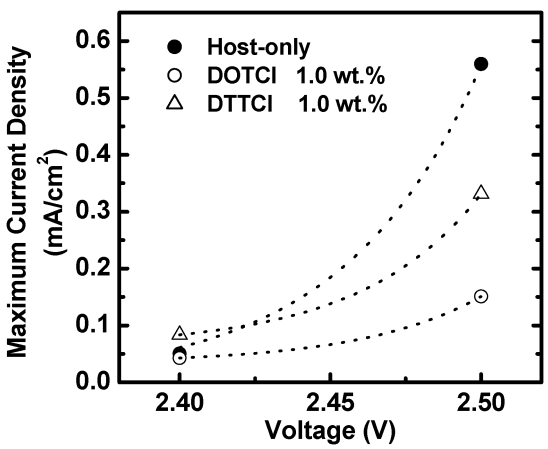

Fig. 9 Maximum current density *vs.* voltage characteristics for the host-only and the host–guest LECs doped with DOTCI (1.0 wt%) and DTTCI (1.0 wt%).

Furthermore, deteriorated device efficiencies of the host–guest LECs doped with a higher guest concentration, which leads to more significant direct carrier trapping, also confirm direct formation of triplet excitons on the guests (Table 1). Hence, direct carrier trapping due to the large energy offsets between the energy levels of the host and the guest molecules (Fig. 6) would play an important role in degradation of device efficiency of phosphorescent sensitized fluorescent LECs. Further studies of appropriate host–guest combinations, *e.g.*, utilizing a host with a smaller energy gap to reduce host–guest energy level offsets and thus to suppress direct carrier trapping on the guest, may be beneficial to further enhancing device efficiencies of phosphorescent sensitized fluorescent NIR LECs.

Conclusions

In summary, we have reported phosphorescent sensitized fluorescent NIR LECs utilizing a phosphorescent CTMC $[Ir(ppy)_2(dasb)]^+(PF_6^-)$ as the host and two fluorescent ionic NIR emitting dyes DOTCI and DTTCI as the guests. PL measurements show that the host–guest films containing low guest concentrations effectively quench host emission due to efficient host–guest energy transfer. EL measurements reveal that the EL spectra of the NIR LECs doped with DOTCI and DTTCI center at *ca.* 730 and 810 nm, respectively. Moreover, the DOTCI and DTTCI doped NIR LECs achieve peak EQE (power efficiency) up to 0.80% (5.65 mW W^{-1}) and 1.24% (7.84 mW W^{-1}), respectively. The device efficiencies achieved are among the highest reported for NIR LECs and thus confirm that phosphorescent sensitized fluorescence is useful for achieving efficient NIR LECs.

Acknowledgements

The authors gratefully acknowledge the financial support from the National Science Council of Taiwan.

References

1 G. Qian and Z. Y. Wang, *Chem.–Asian J.*, 2010, **5**, 1006.
2 Q. Pei, G. Yu, C. Zhang, Y. Yang and A. J. Heeger, *Science*, 1995, **269**, 1086.
3 Q. Pei, Y. Yang, G. Yu, C. Zhang and A. J. Heeger, *J. Am. Chem. Soc.*, 1996, **118**, 3922.
4 J. K. Lee, D. S. Yoo, E. S. Handy and M. F. Rubner, *Appl. Phys. Lett.*, 1996, **69**, 1686.
5 H. Rudmann, S. Shimada and M. F. Rubner, *J. Am. Chem. Soc.*, 2002, **124**, 4918.
6 G. Kalyuzhny, M. Buda, J. McNeill, P. Barbara and A. J. Bard, *J. Am. Chem. Soc.*, 2003, **125**, 6272.
7 J. D. Slinker, D. Bernards, P. L. Houston, H. D. Abruña, S. Bernhard and G. G. Malliaras, *Chem. Commun.*, 2003, 2392.
8 H. Rudmann, S. Shimada and M. F. Rubner, *J. Appl. Phys.*, 2003, **94**, 115.
9 J. D. Slinker, A. A. Gorodetsky, M. S. Lowry, J. Wang, S. Parker, R. Rohl, S. Bernhard and G. G. Malliaras, *J. Am. Chem. Soc.*, 2004, **126**, 2763.
10 S. T. Parker, J. D. Slinker, M. S. Lowry, M. P. Cox, S. Bernhard and G. G. Malliaras, *Chem. Mater.*, 2005, **17**, 3187.
11 A. R. Hosseini, C. Y. Koh, J. D. Slinker, S. Flores-Torres, H. D. Abruña and G. G. Malliaras, *Chem. Mater.*, 2005, **17**, 6114.
12 A. B. Tamayo, S. Garon, T. Sajoto, P. I. Djurovich, I. M. Tsyba, R. Bau and M. E. Thompson, *Inorg. Chem.*, 2005, **44**, 8723.
13 H. J. Bolink, L. Cappelli, E. Coronado and P. Gaviña, *Inorg. Chem.*, 2005, **44**, 5966.

14 Q. Zhang, Q. Zhou, Y. Cheng, L. Wang, D. Ma, X. Jing and F. Wang, *Adv. Funct. Mater.*, 2006, **16**, 1203.
15 H.-C. Su, F.-C. Fang, T.-Y. Hwu, H.-H. Hsieh, H.-F. Chen, G.-H. Lee, S.-M. Peng, K.-T. Wong and C.-C. Wu, *Adv. Funct. Mater.*, 2007, **17**, 1019.
16 H.-C. Su, C.-C. Wu, F.-C. Fang and K.-T. Wong, *Appl. Phys. Lett.*, 2006, **89**, 261118.
17 J. D. Slinker, J. Rivnay, J. S. Moskowitz, J. B. Parker, S. Bernhard, H. D. Abruña and G. G. Malliaras, *J. Mater. Chem.*, 2007, **17**, 2976.
18 L. He, L. Duan, J. Qiao, R. Wang, P. Wei, L. D. Wang and Y. Qiu, *Adv. Funct. Mater.*, 2008, **18**, 2123.
19 H.-C. Su, H.-F. Chen, F.-C. Fang, C.-C. Liu, C.-C. Wu, K.-T. Wong, Y.-H. Liu and S.-M. Peng, *J. Am. Chem. Soc.*, 2008, **130**, 3413.
20 H. J. Bolink, E. Coronado, R. D. Costa, N. Lardiés and E. Ortí, *Inorg. Chem.*, 2008, **47**, 9149.
21 H.-C. Su, H.-F. Chen, C.-C. Wu and K.-T. Wong, *Chem.–Asian J.*, 2008, **3**, 1922.
22 S. Xun, J. Zhang, X. Li, D. Ma and Z. Y. Wang, *Synth. Met.*, 2008, **158**, 484.
23 L. He, J. Qiao, L. Duan, G. F. Dong, D. Q. Zhang, L. D. Wang and Y. Qiu, *Adv. Funct. Mater.*, 2009, **19**, 2950.
24 H. J. Bolink, E. Coronado, R. D. Costa, P. Gaviña, E. Ortí and S. Tatay, *Inorg. Chem.*, 2009, **48**, 3907.
25 M. Mydlak, C. Bizzarri, D. Hartmann, W. Sarfert, G. Schmid and L. De Cola, *Adv. Funct. Mater.*, 2010, **20**, 1812.
26 H.-C. Su, Y.-H. Lin, C.-H. Chang, H.-W. Lin, C.-C. Wu, F.-C. Fang, H.-F. Chen and K.-T. Wong, *J. Mater. Chem.*, 2010, **20**, 5521.
27 H.-F. Chen, K.-T. Wong, Y.-H. Liu, Y. Wang, Y.-M. Cheng, M.-W. Chung, P.-T. Chou and H.-C. Su, *J. Mater. Chem.*, 2011, **21**, 768.
28 H.-C. Su, H.-F. Chen, Y.-C. Shen, C.-T. Liao and K.-T. Wong, *J. Mater. Chem.*, 2011, **21**, 9653.
29 S. Wang, X. Li, S. Xun, X. Wan and Z. Y. Wang, *Macromolecules*, 2006, **39**, 7502.
30 M. A. Baldo, M. E. Thompson and S. R. Forrest, *Nature*, 2000, **403**, 750.
31 T. Förster, *Discuss. Faraday Soc.*, 1959, **27**, 7.
32 D. L. Dexter, *J. Chem. Phys.*, 1953, **21**, 836.
33 P. F. Aramendia, R. M. Negri and E. S. Roman, *J. Phys. Chem.*, 1994, **98**, 3165.
34 D. W. McCamant, P. Kukura and R. A. Mathies, *Appl. Spectrosc.*, 2003, **57**, 1317.
35 J. L. Bredas, R. Silbey, D. S. Boudreux and R. R. Chance, *J. Am. Chem. Soc.*, 1983, **105**, 6555.
36 B. Park, Y. H. Huh, H. G. Jeon, C. H. Park, T. K. Kang, B. H. Kim and J. Park, *J. Appl. Phys.*, 2010, **108**, 094506.
37 K. W. Lee, J. D. Slinker, A. A. Gorodetsky, S. Flores-Torres, H. D. Abruña, P. L. Houston and G. G. Malliaras, *Phys. Chem. Chem. Phys.*, 2003, **5**, 2706.
38 V. Bulovic, A. Shoustikov, M. A. Baldo, E. Bose, V. G. Kozlov, M. E. Thompson and S. R. Forrest, *Chem. Phys. Lett.*, 1998, **287**, 455.

